



A spline collocation method for a fractional mobile–immobile equation with variable coefficients

Xuehua Yang¹ · Haixiang Zhang¹ · Qiong Tang¹

Received: 2 April 2019 / Revised: 2 November 2019 / Accepted: 12 November 2019 /
Published online: 21 November 2019
© SBMAC - Sociedade Brasileira de Matemática Aplicada e Computacional 2019

Abstract

The Crank–Nicolson orthogonal spline collocation (OSC) methods are considered for approximate solution of the variable coefficient fractional mobile–immobile equation. The convection, diffusion, and reaction coefficients can depend on both the spatial and temporal variables, simultaneously. Combining with Crank–Nicolson scheme and weighted and shifted Grünwald difference approximation in time, we establish OSC method in space. It is proved that our proposed fully methods are of optimal order in certain H_j ($j = 0, 1$) norms. Moreover, we derive L^∞ estimates in space. Numerical results are also provided to verify our proposed algorithm.

Keywords Fractional convection diffusion equation · Collocation method · Variable coefficient · Finite-difference method · Stability and convergence

Mathematics Subject Classification 65M60 · 26A33

1 Introduction

In this paper, we consider the following fractional-order mobile–immobile equation with variable coefficients:

Communicated by Vasily E. Tarasov.

The work was supported by National Natural Science Foundation of China (11701168, 11601144), Hunan Provincial Natural Science Foundation of China (2018JJ3108, 2018JJ3109, 2018JJ4062), Scientific Research Fund of Hunan Provincial Education Department (18B304, YB2016B033), and China Postdoctoral Science Foundation (2018M631403).

✉ Haixiang Zhang
hassenzhang@163.com

Xuehua Yang
hunanshidayang@163.com

Qiong Tang
zzgxyssx@163.com

¹ College of Sciences, Hunan University of Technology, Zhuzhou 412008, China

$${}_0^C D_t^\alpha u + u_t + \mathcal{L}u = f(x, y, t), \quad (x, y, t) \in \Omega_T \equiv \Omega \times (0, T], \tag{1.1}$$

$$u(x, y, 0) = u_0(x, y), \quad (x, y) \in \Omega, \tag{1.2}$$

$$u(x, y, t) = 0, \quad (x, y, t) \in \partial\Omega \times (0, T]. \tag{1.3}$$

where $\Omega \subset \mathbb{R}^2$ is bounded convex polygonal domain with boundary $\partial\Omega$, and f and u_0 are given functions. $\mathcal{L}u = \mathcal{L}_1 u + \mathcal{L}_2 u$, $\mathcal{L}_1 u = -p_1(x, y, t)u_{xx} + q_1(x, y, t)u_x + r(x, y, t)u$, and $\mathcal{L}_2 u = -p_2(x, y, t)u_{yy} + q_2(x, y, t)u_y$. There exist positive constants p_{\min}, p_{\max} , such that $0 < p_{\min} \leq p_1(x, y, t), p_2(x, y, t) \leq p_{\max}$. Herein, we consider operator \mathcal{L} in the non-divergence forms rather than in the divergence forms, because the non-divergence forms are more natural for OSC spatial discretization. The Caputo fractional derivative ${}_0^C D_t^\alpha$ is defined by:

$${}_0^C D_t^\alpha u(\cdot, t) = \frac{1}{\Gamma(1-\alpha)} \int_0^t \frac{\partial u(\cdot, s)}{\partial s} \frac{ds}{(t-s)^\alpha}, \quad 0 < \alpha < 1. \tag{1.4}$$

The fractional-order mobile-immobile equations are a type of second order PDEs, which describe a family of problems including heat diffusion and ocean acoustic propagation in mathematical systems with the time variable t and behaves like heat diffusing through a solid. The time drift term u_t is added to exhibit the motion time and thus helps to distinguish the status of particles conveniently. The model is the limiting equation which control continuous time random walks with heavy-tailed random waiting times. Hence, it is difficult or infeasible to find the analytical solution of this equations in most cases, and then to find its numerical solutions become more necessary. Most of previous works concentrate on constant coefficient problems Jiang (2015), Wei (2017, 2018), Chen et al. (2016), He and Pan (2017, 2018), and Liu et al. (2015). For variable coefficient, Cui (2015) studied the time fractional convection-diffusion reaction equation with variable coefficients by the compact exponential scheme. Wang et al. (2019) provide a novel high-order approximate scheme for time-fractional 2D diffusion equations with variable coefficient. Liu et al. (2012) analyzed novel and efficient numerical methods for a class of fractional advection-dispersion models, including the mobile/immobile time-fractional advection-dispersion model with a Caputo fractional derivative. Subsequently, Liu et al. (2014) constructed an RBF meshless method for a fractal mobile-immobile transport model. Zhang et al. (2013) described an implicit Euler approximation for the time-variable fractional-order mobile-immobile advection-dispersion model. Recently, Liu et al. Liu and Li (2018) introduced the Crank-Nicolson finite-difference scheme to solve a time-variable fractional-order mobile-immobile advection-dispersion equation, and proved a priori estimates of discrete L^2 -norm.

Published articles on numerical methods for fractional mobile-immobile convection-subdiffusion equation with variable coefficients are still sparse. This motivates us to consider high accuracy numerical schemes for solving them. The current work is devoted to deriving a high-order scheme by combining Crank-Nicolson and weighted and shifted Grünwald difference approximation for time derivative and OSC scheme for space. There have been many earlier research papers discussing OSC schemes for steady and/or unsteady convection-diffusion equations of integer order, e.g., Bialecki (1998), Bialecki and Fernandes (1993), Fernandes and Fairweather (1993), Yan and Fairweather (1992), Zhang et al. (2019), and Yang et al. (2019). However, numerical approximation referring OSC method for fractional-order convection-subdiffusion equations with variable coefficients is still at an early stage of development. Thus, it is important and necessary to develop efficient numerical methods to solve them.

The structure of the paper is organized as follows. In Sect. 2, the Crank-Nicolson OSC method is derived. The heart of our paper is Sect. 3, where we prove the stability and conver-

gence in certain H_j ($j = 0, 1$) norms for proposed scheme. In Sect. 4, numerical experiments are given; at last, some conclusions are drawn in Sect. 5.

2 The Crank–Nicolson OSC scheme

2.1 Preliminaries

Let N_x, N_y , and N be some positive integer, the collection of spatial quasi-uniform Percell and Wheeler (1980) mesh of Ω defined by $\delta \equiv \delta_x \times \delta_y, \delta_x : 0 = x_0 < x_1 < \dots < x_{N_x} = 1, \delta_y : 0 = y_0 < y_1 < \dots < y_{N_y} = 1, 1 \leq k \leq N_x, 1 \leq l \leq N_y$.

Denote by $\mathcal{M}_r(\delta) \equiv \mathcal{M}(r, \delta_x) \otimes \mathcal{M}(r, \delta_y)$ a space of piecewise polynomials in x and $y, \mathcal{M}(r, \delta_x) = \{u|u \in C^1([0, 1]), u|_{[x_{k-1}, x_k]} \in P_r, u(0) = u(1) = 0\}$, and P_r denotes the space of all polynomials of degree less than or equal to r . With $\mathcal{M}(r, \delta_y)$ defined similarly.

Let $\{\lambda_k\}_{k=1}^{r-1}$ and $\{\omega_k\}_{k=1}^{r-1}$ be the nodes and weights of the $(r - 1)$ -point Gauss quadrature rule on $[0, 1]$. In domain Ω , we define Gauss collocation points set: $\Lambda_r \equiv \{\xi|\xi = (\xi^x, \xi^y), \xi^x \in \Lambda_x, \xi^y \in \Lambda_y\}, \Lambda_x = \{x_{i-1} + \lambda_k h_i^x\}_{i,k=1}^{N_x, r-1}, h_k^x = x_k - x_{k-1}$. With Λ_y defined similarly.

At last, the discrete inner product and norm are defined by:

$$\langle U, V \rangle = \sum_{i=1}^{N_x} \sum_{j=1}^{N_y} h_i^x h_j^y \sum_{k=1}^{r-1} \sum_{l=1}^{r-1} \omega_k \omega_l (UV)(\xi_{i,k}^x, \xi_{j,l}^y), \quad U, V \in \mathcal{M}_r(\delta),$$

$$\|V\|_{\mathcal{M}_r}^2 = \langle V, V \rangle, \quad V \in \mathcal{M}_r(\delta).$$

2.2 Construction of OSC scheme

In this subsection, we will consider Crank–Nicolson OSC scheme for approximating the solution of problem (1.1). Let temporal domain $[0, T]$ be divided by the partition $\{t_k\}_{k=0}^K$ with $t_k = k\tau$, and $\tau = T/K$. Next, we introduce some difference quotient notations:

$$V^n(\cdot, \cdot) = V(\cdot, \cdot, t_n), \delta_t V^{n+1} = \frac{V^{n+1} - V^n}{\tau}, \quad V^{n+\frac{1}{2}} = \frac{1}{2}(V^{n+1} + V^n).$$

We first consider the weighted and shifted Grünwald–Letnikon approximation Tian et al. (2015) and Wang and Vong (2014) for ${}^C D_t^\alpha u(\cdot, t)$:

$${}^C D_t^\alpha u(x, y, t_{n+1}) = \tau^{-\alpha} \sum_{k=0}^{n+1} \lambda_k^{(\alpha)} u(x, y, t_{n+1-k}) + R_{(\alpha)}^{n+1}, \tag{2.1}$$

where

$$\begin{cases} \lambda_k^{(\alpha)} = -\frac{\alpha}{2} g_{k-1}^{(\alpha)} + \frac{2+\alpha}{2} g_k^{(\alpha)}, & k = 1, 2, 3, \dots; \\ \lambda_0^{(\alpha)} = \frac{2+\alpha}{2} g_0^{(\alpha)}, & k = 0. \end{cases} \tag{2.2}$$

and

$$g_k^{(\alpha)} = \left(1 - \frac{\alpha + 1}{k}\right) g_{k-1}^{(\alpha)}, \quad g_0^{(\alpha)} = 1.$$

It can be checked directly for $0 < \alpha < 1$ that the coefficients $\{g_k^{(\alpha)}\}_{k=0}^\infty$ and $\{\lambda_k^{(\alpha)}\}_{k=0}^\infty$ satisfy the following properties:

$$\begin{cases} g_1^{(\alpha)} = -\alpha < 0, & g_2^{(\alpha)} \leq g_3^{(\alpha)} \leq g_4^{(\alpha)} \leq \dots \leq 0; \\ \sum_{k=1}^\infty g_k^{(\alpha)} = -1, & \sum_{k=0}^n g_k^{(\alpha)} \geq 0, \quad n \geq 1; \\ \lambda_0^{(\alpha)} = 1 + \frac{\alpha}{2} > 0, & \sum_{k=0}^{n+1} |\lambda_k^{(\alpha)}| \leq 2\alpha + 2. \end{cases} \tag{2.3}$$

Moreover, for any real vector $(w_1, w_2, \dots, w_k)^T \in \mathbb{R}^k$, it holds that:

$$\sum_{n=0}^{k-1} \left(\sum_{p=0}^n \lambda_p^{(\alpha)} w_{n+1-p} \right) w_{n+1} \geq 0, \quad k = 1, 2, \dots \tag{2.4}$$

For the proof, see Wang and Vong (2014).

The estimate of $R_{n+1}^{(\alpha)}$ can be found in Tian et al. (2015), and satisfies:

$$\left| R_{(\alpha)}^{n+1} \right| \leq C \tau^2 \left\| \mathfrak{F}[{}_0^{RL} D_t^{\alpha+2} u](\omega) \right\|_{L^1}, \tag{2.5}$$

where \mathfrak{F} denotes the Fourier transform symbol, and $u \in C^2, {}_0^{RL} D_t^{\alpha+2} u$, and its Fourier transform belong to $L^1(\mathbb{R})$.

Therefore, using the approximate formula (2.1), the Crank–Nicolson OSC scheme for Eq. (1.1) consists in finding $\{u_h^n\}_{n=0}^K \subset \mathcal{M}_r(\delta)$, such that, for all $\xi \in \Lambda_r$:

$$\left\{ \delta_t u_h^{n+1} + \frac{\tau^{-\alpha}}{2} \left[\sum_{k=0}^{n+1} \lambda_k^{(\alpha)} u_h^{n+1-k} + \sum_{k=0}^n \lambda_k^{(\alpha)} u_h^{n-k} \right] + \mathcal{L}^{n+\frac{1}{2}} u_h^{n+\frac{1}{2}} \right\} (\xi) = f^{n+\frac{1}{2}}(\xi),$$

where $\mathcal{L}^{n+\frac{1}{2}}$ and $f^{n+\frac{1}{2}}$ denote the operator $\mathcal{L}(t)$ and the function $f(t)$, respectively, evaluated at $t = t_{n+\frac{1}{2}}$. For the stability and error analysis, we rewrite the above equation in the equivalent form:

$$\begin{aligned} \langle \delta_t u_h^{n+1}, v_h \rangle + \langle \mathcal{L}^{n+\frac{1}{2}} u_h^{n+\frac{1}{2}}, v_h \rangle &= -\tau^{-\alpha} \sum_{k=0}^n \lambda_k^{(\alpha)} \langle u_h^{n-k+\frac{1}{2}}, v_h \rangle \\ &\quad - \frac{\tau^{-\alpha}}{2} \lambda_{n+1}^{(\alpha)} \langle u_h^0, v_h \rangle + \langle f^{n+\frac{1}{2}}, v_h \rangle, \quad v_h \in \mathcal{M}_r(\delta), \quad 0 \leq n \leq K-1, \end{aligned} \tag{2.6}$$

where, for convenience, we have omitted the dependence of $u^{n+1}(\xi)$ on (ξ) in the above equation.

3 Analysis of the Crank–Nicolson OSC scheme

To analyze the convergence of fully discrete scheme (2.6), we begin with the following Lemma.

Lemma 3.1 Bialecki and Fernandes (1993) *If $\mathcal{L} = \mathcal{L}_1 + \mathcal{L}_2$, and assume $p_1 \in C^{5,0,0}(\Omega_T)$, $p_2 \in C^{0,5,0}(\Omega_T)$, $q_1, q_2, r \in C(\Omega_T)$. Also assume that $p_i, i = 1, 2$ satisfy the Lipschitz*

condition with respect to t , that is, for $(x, y) \in \Omega, t_1, t_2 \in (0, T]$, there is a constant $C > 0$, such that

$$|p_i(x, y, t_1) - p_i(x, y, t_2)| \leq C|t_1 - t_2|, \quad i = 0, 1,$$

then we can show that:

$$\langle \mathcal{L}(t)W, V \rangle = A_0(t; W, V) + A_1(t; W, V), \quad t \in (0, T], W, V \in \mathcal{M}_r(\delta), \quad (3.1)$$

where $A_i(t; \cdot, \cdot), t \in (0, T], i = 0, 1$, are real-valued bilinear forms on $\mathcal{M}_r(\delta) \times \mathcal{M}_r(\delta)$ for all $t \in (0, T], W, V \in \mathcal{M}_r(\delta)$, p_{min}, p_{max} , and C are positive constants, we have:

$$(1) A_0(t; W, V) = A_0(t; V, W); \quad (3.2)$$

$$(2) p_{min} \langle -\Delta W, W \rangle \leq A_0(t; W, W) \leq p_{max} \langle -\Delta W, W \rangle; \quad (3.3)$$

$$(3) |A_0(t_1; W, W) - A_0(t_2; W, W)| \leq C|t_1 - t_2| \langle -\Delta W, W \rangle; \quad (3.4)$$

$$(4) A_1(t_1; W, V) \leq C_\varrho \langle -\Delta W, W \rangle^{\frac{1}{2}} \|V\|_{\mathcal{M}_r}; \quad (3.5)$$

where

$$\varrho = \|q_1\|_{C(\Omega_T)} + \|q_2\|_{C(\Omega_T)} + \|r\|_{C(\Omega_T)} + \max_{1 \leq i \leq 5} \left(\left\| \frac{\partial^i p_1}{\partial x^i} \right\|_{C(\Omega_T)}, \left\| \frac{\partial^i p_2}{\partial y^i} \right\|_{C(\Omega_T)} \right).$$

For the proof, see Bialecki and Fernandes (1993), Lemma 3.2.

3.1 L^2 stability analysis

The L^2 stability of Crank–Nicolson OSC scheme (2.6) is given in the following theorem.

Theorem 3.2 *The Crank–Nicolson OSC scheme (2.6) is stable with respect to L^2 norm. Specifically, for $u_h^m \in \mathcal{M}_r(\delta)$, it holds:*

$$\|u_h^m\|_{\mathcal{M}_r}^2 \leq C \left(\tau^{1-\alpha} \|u_h^0\|_{\mathcal{M}_r}^2 + \tau \sum_{n=0}^{m-1} \|f^{n+\frac{1}{2}}\|_{\mathcal{M}_r}^2 \right), \quad 1 \leq m \leq K. \quad (3.6)$$

Proof Taking $v_h = u_h^{n+\frac{1}{2}}$ in (2.6), for $0 \leq n \leq K - 1$, we obtain:

$$\begin{aligned} & \langle \delta_t u_h^{n+1}, u_h^{n+\frac{1}{2}} \rangle + \langle \mathcal{L}^{n+\frac{1}{2}} u_h^{n+\frac{1}{2}}, u_h^{n+\frac{1}{2}} \rangle \\ &= -\tau^{-\alpha} \sum_{k=0}^n \lambda_k^{(\alpha)} \langle u_h^{n-k+\frac{1}{2}}, u_h^{n+\frac{1}{2}} \rangle \\ & \quad - \frac{\tau^{-\alpha}}{2} \lambda_{n+1}^{(\alpha)} \langle u_h^0, u_h^{n+\frac{1}{2}} \rangle + \langle f^{n+\frac{1}{2}}, u_h^{n+\frac{1}{2}} \rangle. \end{aligned} \quad (3.7)$$

Since

$$\left\langle \delta_t u_h^{n+1}, u_h^{n+\frac{1}{2}} \right\rangle = \frac{1}{2} \delta_t \|u_h^{n+1}\|_{\mathcal{M}_r}^2, \quad (3.8)$$

it follows from (3.1) of Lemma 3.1 that:

$$\left\langle \mathcal{L}^{n+\frac{1}{2}} u_h^{n+\frac{1}{2}}, u_h^{n+\frac{1}{2}} \right\rangle = A_0 \left(t_{n+\frac{1}{2}}; u_h^{n+\frac{1}{2}}, u_h^{n+\frac{1}{2}} \right) + A_1 \left(t_{n+\frac{1}{2}}; u_h^{n+\frac{1}{2}}, u_h^{n+\frac{1}{2}} \right), \quad (3.9)$$

from Eq. (3.4) of Fernandes and Fairweather (1993), we have:

$$\left\langle -\Delta u_h^{n+\frac{1}{2}}, u_h^{n+\frac{1}{2}} \right\rangle \geq C \left\| \nabla u_h^{n+\frac{1}{2}} \right\|^2 \geq 0. \tag{3.10}$$

Furthermore, using (3.3) and (3.5), we have:

$$\begin{aligned} & \left\langle \mathcal{L}^{n+\frac{1}{2}} u_h^{n+\frac{1}{2}}, u_h^{n+\frac{1}{2}} \right\rangle \\ & \geq p_{\min} \left\langle -\Delta u_h^{n+\frac{1}{2}}, u_h^{n+\frac{1}{2}} \right\rangle - C_\varrho \left\langle -\Delta u_h^{n+\frac{1}{2}}, u_h^{n+\frac{1}{2}} \right\rangle^{\frac{1}{2}} \|u_h^{n+\frac{1}{2}}\|_{\mathcal{M}_r} \\ & \geq p_{\min} \|\nabla u_h^{n+\frac{1}{2}}\|^2 - C_\varrho \|\nabla u_h^{n+\frac{1}{2}}\| \|u_h^{n+\frac{1}{2}}\|_{\mathcal{M}_r} \\ & \geq \frac{p_{\min}}{2} \|\nabla u_h^{n+\frac{1}{2}}\|^2 - C \|u_h^{n+\frac{1}{2}}\|_{\mathcal{M}_r}^2; \end{aligned} \tag{3.11}$$

on substituting (3.8) and (3.11) into (3.7), multiplying the result equation by 2τ , and then summing from $n = 0$ to $n = m - 1$, $1 \leq m \leq K$, we obtain:

$$\begin{aligned} & \|u_h^m\|_{\mathcal{M}_r}^2 + \tau p_{\min} \sum_{n=0}^{m-1} \|\nabla u_h^{n+\frac{1}{2}}\|^2 \\ & \leq \|u_h^0\|_{\mathcal{M}_r}^2 + C\tau \sum_{n=0}^{m-1} \|u_h^{n+\frac{1}{2}}\|^2 - 2\tau^{1-\alpha} \sum_{n=0}^{m-1} \sum_{k=0}^n \lambda_k^{(\alpha)} \left\langle u_h^{n-k+\frac{1}{2}}, u_h^{n+\frac{1}{2}} \right\rangle \\ & \quad - \tau^{1-\alpha} \sum_{n=0}^{m-1} \lambda_{n+1}^{(\alpha)} \left\langle u_h^0, u_h^{n+\frac{1}{2}} \right\rangle + 2\tau \sum_{n=0}^{m-1} \left\langle f^{n+\frac{1}{2}}, u_h^{n+\frac{1}{2}} \right\rangle. \end{aligned} \tag{3.12}$$

It follows from (2.4), we obtain:

$$-2\tau^{1-\alpha} \sum_{n=0}^{m-1} \sum_{k=0}^n \lambda_k^{(\alpha)} \left\langle u_h^{n-k+\frac{1}{2}}, u_h^{n+\frac{1}{2}} \right\rangle \leq 0,$$

dropping the non-positive the third term on the RHS of (3.12), then applying the Cauchy–Schwarz inequality and Young’s inequality to the last two terms on the RHS of the resulting expression, and noticing $\|u_h^{n+\frac{1}{2}}\|_{\mathcal{M}_r} \leq \frac{1}{2}(\|u_h^{n+1}\|_{\mathcal{M}_r} + \|u_h^n\|_{\mathcal{M}_r})$, we have:

$$\begin{aligned} & \|u_h^m\|_{\mathcal{M}_r}^2 + C\tau \sum_{n=0}^{m-1} \|\nabla u_h^{n+\frac{1}{2}}\|^2 \leq C \left(\|u_h^0\|_{\mathcal{M}_r}^2 \right. \\ & \quad \left. + \tau^{1-\alpha} \sum_{n=0}^{m-1} |\lambda_{n+1}^{(\alpha)}| \|u_h^0\|_{\mathcal{M}_r}^2 + \tau \sum_{n=0}^{m-1} \|f^{n+\frac{1}{2}}\|_{\mathcal{M}_r}^2 \right) + C\tau \sum_{n=0}^{m-1} \|u_h^n\|^2. \end{aligned} \tag{3.13}$$

Using the discrete Gronwall lemma, (2.3), and (3.13), we complete the proof of Theorem 3.2. □

3.2 H^1 stability analysis

In the following theorem, we derive the H^1 stability of the Crank–Nicolson OSC scheme (2.6).

Theorem 3.3 *The Crank–Nicolson OSC scheme (2.6) is stable with respect to H^1 norm. Specifically, for $u_h^m \in \mathcal{M}_r(\delta)$, $1 \leq m \leq K$, it holds:*

$$\|\nabla u_h^m\|^2 \leq C \left(\|\nabla u_h^0\|^2 + \tau^{1-\alpha} \|u_h^0\|_{\mathcal{M}_r}^2 + \tau \sum_{n=0}^{m-1} \|f^{n+\frac{1}{2}}\|_{\mathcal{M}_r}^2 \right). \tag{3.14}$$

Proof Setting $v_h = \delta_t u_h^{n+1}$ in (2.6), for $0 \leq n \leq K - 1$, we obtain:

$$\begin{aligned} & \|\delta_t u_h^{n+1}\|_{\mathcal{M}_r}^2 + \left\langle \mathcal{L}^{n+\frac{1}{2}} u_h^{n+\frac{1}{2}}, \delta_t u_h^{n+1} \right\rangle \\ &= -\tau^{-\alpha} \sum_{k=0}^n \lambda_k^{(\alpha)} \left\langle u_h^{n-k+\frac{1}{2}}, \delta_t u_h^{n+1} \right\rangle \\ & \quad - \frac{\tau^{-\alpha}}{2} \lambda_{n+1}^{(\alpha)} \left\langle u_h^0, \delta_t u_h^{n+1} \right\rangle + \left\langle f^{n+\frac{1}{2}}, \delta_t u_h^{n+1} \right\rangle. \end{aligned} \tag{3.15}$$

First, we have to handle the first term on RHS of (3.15) as follows:

$$\begin{aligned} & -\tau^{-\alpha} \sum_{k=0}^n \lambda_k^{(\alpha)} \left\langle u_h^{n-k+\frac{1}{2}}, \delta_t u_h^{n+1} \right\rangle \\ &= -\tau^{-\alpha} \sum_{k=0}^n \lambda_k^{(\alpha)} \left\langle \frac{u_h^{n-k+1} + u_h^{n-k}}{2}, \frac{u_h^{n+1} - u_h^n}{\tau} \right\rangle \\ &= -\frac{\tau^{1-\alpha}}{2} \sum_{k=0}^n \lambda_k^{(\alpha)} \left\langle \delta_t u_h^{n-k+1}, \delta_t u_h^{n+1} \right\rangle - \tau^{-\alpha} \sum_{k=0}^n \lambda_k^{(\alpha)} \left\langle u_h^{n-k}, \delta_t u_h^{n+1} \right\rangle. \end{aligned} \tag{3.16}$$

Now, we handle the second term on LHS of (3.15), following (3.1) of Lemma 3.1, we have:

$$\begin{aligned} & \left\langle \mathcal{L}^{n+\frac{1}{2}} u_h^{n+\frac{1}{2}}, \delta_t u_h^{n+1} \right\rangle \\ &= A_0(t_{n+\frac{1}{2}}; u_h^{n+\frac{1}{2}}, \delta_t u_h^{n+1}) + A_1(t_{n+\frac{1}{2}}; u_h^{n+\frac{1}{2}}, \delta_t u_h^{n+1}), \end{aligned} \tag{3.17}$$

since

$$\begin{aligned} & A_0(t_{n+\frac{1}{2}}; u_h^{n+\frac{1}{2}}, \delta_t u_h^{n+1}) \\ &= \frac{1}{2\tau} A_0(t_{n+\frac{1}{2}}; u_h^{n+1} + u_h^n, u_h^{n+1} - u_h^n) \\ &= \frac{1}{2\tau} \left[A_0(t_{n+\frac{1}{2}}; u_h^{n+1}, u_h^{n+1}) - A_0(t_{n-\frac{1}{2}}; u_h^n, u_h^n) \right] \\ & \quad - \frac{1}{2\tau} \left[A_0(t_{n+\frac{1}{2}}; u_h^n, u_h^n) - A_0(t_{n-\frac{1}{2}}; u_h^n, u_h^n) \right] \\ &= \frac{1}{2} \delta_t \left(A_0(t_{n+\frac{1}{2}}; u_h^{n+1}, u_h^{n+1}) \right) - \frac{1}{2} (\delta_t A_0)(t_{n+\frac{1}{2}}; u_h^n, u_h^n); \end{aligned} \tag{3.18}$$

substituting (3.16)–(3.18) into (3.15), multiplying the result equation by 2τ , and then summing from $n = 1$ to $n = m - 1$, $1 \leq m \leq K$, we obtain:

$$\begin{aligned}
 & 2\tau \sum_{n=1}^{m-1} \|\delta_t u_h^{n+1}\|_{\mathcal{M}_r}^2 + A_0(t_{m-\frac{1}{2}}; u_h^m, u_h^m) = A_0(t_{\frac{1}{2}}; u_h^1, u_h^1) \\
 & + \tau \sum_{n=1}^{m-1} (\delta_t A_0)(t_{n+\frac{1}{2}}; u_h^n, u_h^n) - 2\tau \sum_{n=1}^{m-1} A_1(t_{n+\frac{1}{2}}; u_h^{n+\frac{1}{2}}, \delta_t u_h^{n+1}) \\
 & - \tau^{2-\alpha} \sum_{n=1}^{m-1} \sum_{k=0}^n \lambda_k^{(\alpha)} \langle \delta_t u_h^{n-k+1}, \delta_t u_h^{n+1} \rangle \\
 & - 2\tau^{1-\alpha} \sum_{n=1}^{m-1} \sum_{k=0}^n \lambda_k^{(\alpha)} \langle u_h^{n-k}, \delta_t u_h^{n+1} \rangle \\
 & - \tau^{1-\alpha} \sum_{n=1}^{m-1} \lambda_{n+1}^{(\alpha)} \langle u_h^0, \delta_t u_h^{n+1} \rangle + 2\tau \sum_{n=1}^{m-1} \langle f^{n+\frac{1}{2}}, \delta_t u_h^{n+1} \rangle. \tag{3.19}
 \end{aligned}$$

Taking $n = 0$ in (3.15), we obtain:

$$\begin{aligned}
 & \|\delta_t u_h^1\|_{\mathcal{M}_r}^2 + \langle \mathcal{L}^{\frac{1}{2}} u_h^{\frac{1}{2}}, \delta_t u_h^1 \rangle = -\tau^{-\alpha} \lambda_0^{(\alpha)} \langle u_h^1, \delta_t u_h^1 \rangle \\
 & - \frac{\tau^{-\alpha}}{2} \lambda_1^{(\alpha)} \langle u_h^0, \delta_t u_h^1 \rangle + \langle f^{\frac{1}{2}}, \delta_t u_h^1 \rangle, \quad 0 \leq n \leq K - 1; \tag{3.20}
 \end{aligned}$$

following (3.1):

$$\begin{aligned}
 \langle \mathcal{L}^{\frac{1}{2}} u_h^{\frac{1}{2}}, \delta_t u_h^1 \rangle &= \frac{1}{2\tau} \langle \mathcal{L}^{\frac{1}{2}} (u_h^1 + u_h^0), u_h^1 - u_h^0 \rangle \\
 &= \frac{1}{2\tau} \left[A_0(t_{\frac{1}{2}}; u_h^1 + u_h^0, u_h^1 - u_h^0) + A_1(t_{\frac{1}{2}}; u_h^1 + u_h^0, u_h^1 - u_h^0) \right] \\
 &= \frac{1}{2\tau} \left[A_0(t_{\frac{1}{2}}; u_h^1, u_h^1) - A_0(t_{\frac{1}{2}}; u_h^0, u_h^0) \right] + \frac{1}{2\tau} A_1(t_{\frac{1}{2}}; u_h^1 + u_h^0, u_h^1 - u_h^0). \tag{3.21}
 \end{aligned}$$

Furthermore, substituting (3.21) into (3.20), multiplying the resulting expression by 2τ , we have:

$$\begin{aligned}
 & 2\tau \|\delta_t u_h^1\|_{\mathcal{M}_r}^2 + A_0(t_{\frac{1}{2}}; u_h^1, u_h^1) \\
 & = A_0(t_{\frac{1}{2}}; u_h^0, u_h^0) - A_1(t_{\frac{1}{2}}; u_h^1 + u_h^0, u_h^1 - u_h^0) \\
 & - 2\tau^{1-\alpha} \lambda_0^{(\alpha)} \langle u_h^1, \delta_t u_h^1 \rangle - \tau^{1-\alpha} \lambda_1^{(\alpha)} \langle u_h^0, \delta_t u_h^1 \rangle + 2\tau \langle f^{\frac{1}{2}}, \delta_t u_h^1 \rangle; \tag{3.22}
 \end{aligned}$$

adding (3.22)–(3.19), for $1 \leq m \leq K$, we have:

$$\begin{aligned}
 & 2\tau \sum_{n=0}^{m-1} \|\delta_t u_h^{n+1}\|_{\mathcal{M}_r}^2 + A_0(t_{m-\frac{1}{2}}; u_h^m, u_h^m) \\
 & = A_0(t_{\frac{1}{2}}; u_h^0, u_h^0) + \tau \sum_{n=1}^{m-1} (\delta_t A_0)(t_{n+\frac{1}{2}}; u_h^n, u_h^n)
 \end{aligned}$$

$$\begin{aligned}
 & -2\tau \sum_{n=0}^{m-1} A_1(t_{n+\frac{1}{2}}; u_h^{n+\frac{1}{2}}, \delta_t u_h^{n+1}) \\
 & -\tau^{2-\alpha} \sum_{n=1}^{m-1} \sum_{k=0}^n \lambda_k^{(\alpha)} \langle \delta_t u_h^{n-k+1}, \delta_t u_h^{n+1} \rangle \\
 & -2\tau^{1-\alpha} \sum_{n=0}^{m-1} \sum_{k=0}^n \lambda_k^{(\alpha)} \langle u_h^{n-k}, \delta_t u_h^{n+1} \rangle \\
 & -\tau^{1-\alpha} \sum_{n=0}^{m-1} \lambda_{n+1}^{(\alpha)} \langle u_h^0, \delta_t u_h^{n+1} \rangle + 2\tau \sum_{n=0}^{m-1} \langle f^{n+\frac{1}{2}}, \delta_t u_h^{n+1} \rangle. \tag{3.23}
 \end{aligned}$$

It follows from (2.4) that:

$$-\tau^{2-\alpha} \sum_{n=1}^{m-1} \sum_{k=0}^n \lambda_k^{(\alpha)} \langle \delta_t u_h^{n-k+1}, \delta_t u_h^{n+1} \rangle \leq 0; \tag{3.24}$$

using (3.10) and (3.3), we have:

$$A_0(t_{m-\frac{1}{2}}; u_h^m, u_h^m) \geq p_{\min} \|\nabla u_h^m\|^2, \quad A_0(t_{\frac{1}{2}}; u_h^0, u_h^0) \leq p_{\max} \|\nabla u_h^0\|^2; \tag{3.25}$$

using Eq. (3.5) of Fernandes and Fairweather (1993), we have:

$$|(-\Delta u_h^n, u_h^n)| \leq C \|\nabla u_h^n\| \|\nabla u_h^n\|; \tag{3.26}$$

also, using (3.26) and (3.4) in Lemma 3.1, we have:

$$\begin{aligned}
 (\delta_t A_0)(t_{n+\frac{1}{2}}; u_h^n, u_h^n) & \leq \frac{1}{\tau} \left| A_0(t_{n+\frac{1}{2}}; u_h^n, u_h^n) - A_0(t_{n-\frac{1}{2}}; u_h^n, u_h^n) \right| \\
 & \leq C \langle -\Delta u_h^n, u_h^n \rangle \leq C_1 \|\nabla u_h^n\|^2. \tag{3.27}
 \end{aligned}$$

Similarly, using (3.5) in Lemma 3.1 and (3.26), we have:

$$A_1(t_{n+\frac{1}{2}}; u_h^{n+\frac{1}{2}}, \delta_t u_h^{n+1}) \leq C \|\nabla u_h^{n+\frac{1}{2}}\| \|\delta_t u_h^{n+1}\|_{\mathcal{M}_r}. \tag{3.28}$$

Thus, on substituting (3.24)–(3.28) into (3.23), dropping the non-positive the fourth term on the RHS of (3.23), and then applying the Cauchy–Schwarz inequality to the last three terms on the RHS of the resulting expression, we have:

$$\begin{aligned}
 & 2\tau \sum_{n=0}^{m-1} \|\delta_t u_h^{n+1}\|_{\mathcal{M}_r}^2 + p_{\min} \|\nabla u_h^m\|^2 \\
 & \leq p_{\max} \|\nabla u_h^0\|^2 + C\tau \sum_{n=1}^{m-1} \|\nabla u_h^n\|^2 + 2\tau C \sum_{n=0}^{m-1} \|\nabla u_h^{n+\frac{1}{2}}\| \|\delta_t u_h^{n+1}\|_{\mathcal{M}_r} \\
 & \quad + 2\tau^{1-\alpha} \sum_{n=0}^{m-1} \sum_{k=0}^n |\lambda_k^{(\alpha)}| \|u_h^{n-k}\|_{\mathcal{M}_r} \|\delta_t u_h^{n+1}\|_{\mathcal{M}_r} \\
 & \quad + \tau^{1-\alpha} \sum_{n=0}^{m-1} |\lambda_{n+1}^{(\alpha)}| \|u_h^0\|_{\mathcal{M}_r} \|\delta_t u_h^{n+1}\|_{\mathcal{M}_r}
 \end{aligned}$$

$$+2\tau \sum_{n=0}^{m-1} \|f^{n+\frac{1}{2}}\|_{\mathcal{M}_r} \|\delta_t u_h^{n+1}\|_{\mathcal{M}_r}. \tag{3.29}$$

Using (2.3), noticing $\|\nabla u_h^{n+\frac{1}{2}}\| \leq \frac{1}{2}(\|\nabla u_h^{n+1}\| + \|\nabla u_h^n\|)$, $\|u_h^{n-k}\|_{\mathcal{M}_r} \leq C\|\nabla u_h^{n-k}\|_{\mathcal{M}_r}$, applying the Young’s inequality, and simplifying, we have:

$$\begin{aligned} &\tau \sum_{n=0}^{m-1} \|\delta_t u_h^{n+1}\|_{\mathcal{M}_r}^2 + (p_{\min} - C\tau)\|\nabla u_h^m\|^2 \\ &\leq C \left(\|\nabla u_h^0\|^2 + \tau^{1-\alpha} \|u_h^0\|_{\mathcal{M}_r}^2 + 2\tau \sum_{n=0}^{m-1} \|f^{n+\frac{1}{2}}\|_{\mathcal{M}_r}^2 \right) + C\tau \sum_{n=1}^{m-1} \|\nabla u_h^n\|^2; \end{aligned} \tag{3.30}$$

by choosing τ small so that $p_{\min} - C\tau > 0$, and using the discrete Gronwall lemma, we have:

$$\|\nabla u_h^m\|^2 \leq C \left(\|\nabla u_h^0\|^2 + \tau^{1-\alpha} \|u_h^0\|_{\mathcal{M}_r}^2 + 2\tau \sum_{n=0}^{m-1} \|f^{n+\frac{1}{2}}\|_{\mathcal{M}_r}^2 \right), \quad 1 \leq m \leq K.$$

The proof of Theorem 3.3 is completed. □

3.3 Convergence and a superconvergence result

In this subsection, we will consider the convergence of Crank–Nicolson OSC scheme. To analyze the convergence, we need to define an elliptic projection $W: [0, T] \rightarrow \mathcal{M}_r(\delta)$, for $t \in [0, T]$:

$$\langle \mathcal{L}u - \mathcal{L}W, v_h \rangle = 0, \quad \forall v_h \in \mathcal{M}_r(\delta). \tag{3.31}$$

As in Bialecki (1998), for a given function u , Eq. (3.31) has a unique solution $W \in \mathcal{M}_r(\delta)$.

To finish our analysis, we now introduce two lemmas which provide estimates for $u - W$ and its time derivatives.

Lemma 3.4 Bialecki (1998) *Assume $u, \partial u/\partial t \in H^{r+3-j}, j = 0, 1$, and W satisfies (3.31), and then, there exists a constant C , independent of h , such that:*

$$\left\| \frac{\partial^i(u - W)}{\partial t^i} \right\|_{H^j} \leq Ch^{r+1-j} \left\| \frac{\partial^i u}{\partial t^i} \right\|_{H^{r+3-j}}, \quad j = 0, 1, \quad i = 0, 1. \tag{3.32}$$

Lemma 3.5 Bialecki (1998) *Assume $u, \partial u/\partial t \in H^{r+3}$, for $t \in [0, T], l = l_1 + l_2$, we have:*

$$\left\| \frac{\partial^{l+i}(u - W)}{\partial x^{l_1} \partial y^{l_2} \partial t^i} \right\|_{\mathcal{M}_r} \leq Ch^{r+1-l} \left\| \frac{\partial^i u}{\partial t^i} \right\|_{H^{r+3}}, \quad i = 0, 1, \quad 0 \leq l \leq 4. \tag{3.33}$$

Now, we derive an optimal H^ℓ ($\ell = 0, 1$) error estimate.

According to the definition of W in (3.31), for $0 \leq n \leq K$, we assume:

$$\zeta^n = -W^n + u_h^n, \quad \eta^n = -W^n + u^n, \tag{3.34}$$

then

$$u^n - u_h^n = W^n + \eta^n - (\zeta^n + W^n) = \eta^n - \zeta^n. \tag{3.35}$$

It is easy to know that the estimates of η^n are known from Lemmas 3.4 and 3.5. Therefore, to bound $u^n - u_h^n$, we need only to bound ζ^n .

First, from (1.1) and (3.31) at $t = t_{n+\frac{1}{2}}$, (2.6), (3.34), and (3.35), and then for $v_h \in \mathcal{M}_r(\delta)$, we obtain:

$$\begin{aligned} \langle \delta_t \zeta^{n+1}, v_h \rangle + \langle \mathcal{L}^{n+\frac{1}{2}} \zeta^{n+\frac{1}{2}}, v_h \rangle &= -\tau^{-\alpha} \sum_{k=0}^n \lambda_k^{(\alpha)} \langle \zeta^{n-k+\frac{1}{2}}, v_h \rangle \\ &- \frac{\tau^{-\alpha}}{2} \lambda_{n+1}^{(\alpha)} \langle \zeta^0, v_h \rangle + \langle \sigma_{\alpha,u}^{n+\frac{1}{2}}, v_h \rangle, \quad v_h \in \mathcal{M}_r(\delta), \quad 0 \leq n \leq K-1, \end{aligned} \tag{3.36}$$

where

$$\sigma_{\alpha,u}^{n+\frac{1}{2}} = \sigma_1^{n+\frac{1}{2}} + \sigma_2^{n+\frac{1}{2}} + \sigma_3^{n+\frac{1}{2}} + \sigma_4^{n+\frac{1}{2}} + \sigma_5^{n+\frac{1}{2}}, \tag{3.37}$$

and

$$\begin{cases} \sigma_1^{n+\frac{1}{2}} = \delta_t \eta^{n+1}; \\ \sigma_2^{n+\frac{1}{2}} = u_t(t_{n+\frac{1}{2}}) - \delta_t u^{n+1}; \\ \sigma_3^{n+\frac{1}{2}} = L^{n+\frac{1}{2}} \left(W(t_{n+\frac{1}{2}}) - W^{n+\frac{1}{2}} \right); \\ \sigma_4^{n+\frac{1}{2}} = \tau^{-\alpha} \sum_{k=0}^n \lambda_k^{(\alpha)} \eta^{n-k+\frac{1}{2}} + \frac{\tau^{-\alpha}}{2} \lambda_{n+1}^{(\alpha)} \eta^0; \\ \sigma_5^{n+\frac{1}{2}} = R_{(\alpha)}^{n+\frac{1}{2}}. \end{cases}$$

In the following lemma, we derive estimates on $\sigma_{\alpha,u}^{n+\frac{1}{2}}$ that are required to prove the convergence estimates for the proposed Crank–Nicolson OSC scheme in H^ℓ ($\ell = 0, 1$) norms on each time level.

Lemma 3.6 *If $u \in C^{2,0,0} \cap C^{0,2,0} \cap C^{0,0,3}$, ${}^{RL}D_t^\alpha u, u_{tt} \in C([0, T], H^{r+3})$, ${}^{RL}D_t^{\alpha+2}u$ and its Fourier transform belong to $L^1(\mathbb{R})$, for $n = 0, 1, \dots, K-1$, then we have:*

$$\begin{aligned} \left\| \sigma_{\alpha,u}^{n+\frac{1}{2}} \right\|_{\mathcal{M}_r} &\leq Ch^{r+1} \left(\|u_t\|_{C([0,T],H^{r+3})} + \left\| {}^{RL}D_t^\alpha u \right\|_{C([0,T],H^{r+3})} \right) \\ &+ C\tau^2 \left(\|u_{ttt}\|_{C(\Omega_T)} + \|u_{tt}\|_{C^{2,0,0} \cap C^{0,2,0}} \right. \\ &\left. + \|u_{tt}\|_{C([0,T],H^{r+3})} + \left\| \mathfrak{F}[{}^{RL}D_t^{\alpha+2}u](\omega) \right\|_{L^1} \right). \end{aligned} \tag{3.38}$$

Proof Since

$$\begin{aligned} \left\| \sigma_1^{n+\frac{1}{2}} \right\|_{\mathcal{M}_r} &= \frac{1}{\tau} \left\| \int_{t_n}^{t_{n+1}} \frac{\partial \eta}{\partial t}(\cdot, s) ds \right\|_{\mathcal{M}_r} \\ &\leq \frac{1}{\tau} \int_{t_n}^{t_{n+1}} \left\| \frac{\partial \eta}{\partial t}(\cdot, s) \right\|_{\mathcal{M}_r} ds \leq Ch^{r+1} \|u_t\|_{C([0,T],H^{r+3})}. \end{aligned} \tag{3.39}$$

Using Taylor’s theorem with integral remainder, we obtain:

$$\left\| \sigma_2^{n+\frac{1}{2}} \right\|_{\mathcal{M}_r} = \|u_t(t_{n+\frac{1}{2}}) - \delta_t u^{n+1}\|_{\mathcal{M}_r} \leq C\tau^2 \|u_{ttt}\|_{C(\Omega_T)}. \tag{3.40}$$

For the term $\sigma_3^{n+\frac{1}{2}}$, we obtain, on using Taylor’s theorem and the boundedness of the coefficients:

$$\begin{aligned} \|\sigma_3^{n+\frac{1}{2}}\|_{\mathcal{M}_r} &= \|L^{n+\frac{1}{2}}\left(W\left(t_{n+\frac{1}{2}}\right) - W^{n+\frac{1}{2}}\right)\|_{\mathcal{M}_r} \\ &\leq C\tau^2\left\|W\left(t_{n+\frac{1}{2}}\right) - W^{n+\frac{1}{2}}\right\|_{C^{2,0,0}\cap C^{0,2,0}} \\ &\leq C\tau^2\|W_{tt}\|_{C^{2,0,0}\cap C^{0,2,0}}. \end{aligned} \tag{3.41}$$

Since

$$\|W_{tt}\|_{C^{2,0,0}\cap C^{0,2,0}} \leq \|(W - u)_{tt}\|_{C^{2,0,0}\cap C^{0,2,0}} + \|u_{tt}\|_{C^{2,0,0}\cap C^{0,2,0}}, \tag{3.42}$$

then, using Taylor’s theorem and arguments as in (3.39), together with Lemma 3.5 ($l = 2, j = 2$), since $r \geq 3$, it follows on using (Fernandes and Fairweather 1993, Lemma 3.2) that:

$$\begin{aligned} \|\sigma_3^{n+\frac{1}{2}}\|_{\mathcal{M}_r} &\leq C\tau^2\left(\|(W - u)_{tt}\|_{C^{2,0,0}\cap C^{0,2,0}} + \|u_{tt}\|_{C^{2,0,0}\cap C^{0,2,0}}\right) \\ &\leq C\tau^2\left(\|u_{tt}\|_{C^{2,0,0}\cap C^{0,2,0}} + \|u_{tt}\|_{C([0,T],H^{r+3})}\right). \end{aligned} \tag{3.43}$$

By (2.5), we know that:

$$\left\| {}_0^{RL}D_t^\alpha \eta(t_{n+\frac{1}{2}}) - \sigma_4^{n+\frac{1}{2}} \right\|_{\mathcal{M}_r} \leq C\tau^2 \left\| \mathfrak{F}[{}_0^{RL}D_t^{\alpha+2}u](\omega) \right\|_{L^1}.$$

Hence, using Lemma 3.5, we have:

$$\begin{aligned} \left\| \sigma_4^{n+\frac{1}{2}} \right\|_{\mathcal{M}_r}^2 &\leq \left\| {}_0^{RL}D_t^\alpha \eta(t_{n+\frac{1}{2}}) \right\|_{\mathcal{M}_r}^2 + \tau^4 \left\| \mathfrak{F}[{}_0^{RL}D_t^{\alpha+2}u](\omega) \right\|_{L^1}^2 \\ &\leq Ch^{2r+2} \left\| {}_0^{RL}D_t^\alpha u \right\|_{C([0,T],H^{r+3})}^2 + \tau^4 \left\| \mathfrak{F}[{}_0^{RL}D_t^{\alpha+2}u](\omega) \right\|_{L^1}^2. \end{aligned} \tag{3.44}$$

Note that

$$\left\| \sigma_5^{n+\frac{1}{2}} \right\|_{\mathcal{M}_r} = \left\| R_{(\alpha)}^{n+\frac{1}{2}} \right\|_{\mathcal{M}_r} \leq C\tau^2 \left\| \mathfrak{F}[{}_0^{RL}D_t^{\alpha+2}u](\omega) \right\|_{L^1}. \tag{3.45}$$

Applying the triangle inequality to (3.37) and using (3.39)–(3.40) and (3.43)–(3.45) yield (3.38). The proof of the Lemma 3.6 is completed. \square

Convergence estimates for the Crank–Nicolson OSC method (2.6) in the H^ℓ norms, $\ell = 0, 1$, are proved in the following theorem.

Theorem 3.7 *If the hypotheses of Lemma 3.6 are satisfied and suppose that u is the solution of (1.1), and u_h^m ($0 \leq m \leq K$) is the solution of the problem (2.6) with $u_h^0 = W^0$, then there exists a positive constant C , independent of h and τ , such that*

$$\|u(t_m) - u_h^m\|_{H_j} \leq C\left(h^{r+1-j} + \tau^2\right), \quad j = 0, 1, \quad 0 \leq m \leq K. \tag{3.46}$$

Proof We first apply the stability result (3.6) and (3.14)–(3.13) to obtain:

$$\|\zeta^m\|_{\mathcal{M}_r}^2 \leq C\left(\tau^{1-\alpha}\|\zeta^0\|_{\mathcal{M}_r}^2 + \tau\sum_{n=0}^{m-1}\|\sigma_{\alpha,u}^{n+\frac{1}{2}}\|_{\mathcal{M}_r}^2\right), \quad 1 \leq m \leq K, \tag{3.47}$$

and

$$\|\nabla \zeta^m\|^2 \leq C \left(\|\nabla \zeta^0\|^2 + \tau^{1-\alpha} \|\zeta^0\|_{\mathcal{M}_r}^2 + \tau \sum_{n=0}^{m-1} \|\sigma_{\alpha, u}^{n+\frac{1}{2}}\|_{\mathcal{M}_r}^2 \right). \tag{3.48}$$

Since $\zeta^0 = 0$, it follows from Lemma 3.6 that:

$$\|\zeta^m\|_{\mathcal{M}_r} \leq C (h^{r+1} + \tau^2), \quad 1 \leq m \leq K, \tag{3.49}$$

and

$$\|\nabla \zeta^m\| \leq C (h^{r+1} + \tau^2), \quad 1 \leq m \leq K. \tag{3.50}$$

Therefore, (3.46) for $j = 0$ and $j = 1$ is obtained on using the triangle inequality, (3.49) and (3.50), respectively, and (3.32) with $l = 0, j = 0$ and $l = 0, j = 1$, respectively. \square

Remark 3.8 If we choose u_h^0 as the elliptic projection W^0 of u_0 defined in (3.31), then $\zeta^0 = 0$. Hence, from (3.50), we obtain a superconvergence result for $\|\zeta^m\|_{H^1}, 1 \leq m \leq K$, namely:

$$\|\zeta^m\|_{H^1} \leq C (h^{r+1} + \tau^2), \quad 1 \leq m \leq K. \tag{3.51}$$

From Sobolev’s inequality, we obtain, since: $\zeta^m \in \mathcal{M}_r$,

$$\|\zeta^m\|_{L^\infty} \leq C \log \left(\frac{1}{h} \right) \|\nabla \zeta^m\|, \quad 1 \leq m \leq K. \tag{3.52}$$

If the optimal maximum norm estimate for η^m are available, namely:

$$\|\eta^m\|_{L^\infty} \leq Ch^{r+1}, \quad 1 \leq m \leq K. \tag{3.53}$$

Then, on using the triangle inequality, we obtain a quasi-optimal L^∞ error estimate:

$$\|u(t_m) - u_h^m\|_{L^\infty} \leq C \log \left(\frac{1}{h} \right) (h^{r+1} + \tau^2), \quad 1 \leq m \leq K. \tag{3.54}$$

Remark 3.9 If the hypotheses of Lemma 3.6 are satisfied, then (3.46) also holds for $j = 0$ and $j = 1$, and suppose u_h^0 is chosen, so that

$$\|u_0 - u_h^0\|_{H^j} \leq Ch^{r+1-j}, \quad j = 0, 1. \tag{3.55}$$

This is satisfied by the choice $u_h^0 = u_{\mathcal{H}^t}^0$, the Hermite interpolant of u_0 defined in Bialecki (Eq. 2.18, Bialecki 1998).

4 Numerical experiments

In this section, we will present numerical experiments to illustrate our theoretical statements. We used the space of piecewise Hermite bicubics ($r = 3$) with the standard value and scaled slope basis functions Yan and Fairweather (1992) on uniform partitions of $[0, 1]$.

Example 1 We consider the following problem similar to Chen et al. (2016):

$$\begin{cases} u_t + {}_0^C D_t^\alpha u - (2 - \sin(tx))u_{xx} + t \cos(tx)u_x + (2 - \cos(tx))u = f(x, t), \\ u(x, 0) = 0, \quad x \in [0, 1], \\ u(x, t) = 0, \quad t \in (0, 1], \end{cases}$$

Table 1 L^2 and L^∞ errors and convergence rates in spatial and temporal directions with $\tau = h^2$ for Example 1

α	N	L^2 error	Rate	L^∞ error	Rate
$\alpha = 0.15$	5	1.0557e-03		1.5748e-03	
	10	6.3397e-05	4.0576	9.5592e-05	4.0421
	20	3.9234e-06	4.0142	5.9845e-06	3.9976
	40	2.4461e-07	4.0035	3.7306e-07	4.0038
$\alpha = 0.5$	5	1.0371e-03		1.5481e-03	
	10	6.2284e-05	4.0575	9.4104e-05	4.0401
	20	3.8545e-06	4.0142	5.8880e-06	3.9984
	40	2.4031e-07	4.0036	3.6705e-07	4.0037
$\alpha = 0.95$	5	1.0103e-03		1.5112e-03	
	10	6.0667e-05	4.0575	9.1915e-05	4.0393
	20	3.7550e-06	4.0143	5.7503e-06	3.9986
	40	2.3411e-07	4.0036	3.5846e-07	4.0038

and

$$\begin{aligned}
 f(x, t) = & \left(\frac{2}{\Gamma(3 - \alpha)} t^{2-\alpha} + 2t + (2 - \cos(tx))t^2 \right) \frac{\sin(2\pi x)}{(1+x)^2} \\
 & + t^3 \cos(tx) \left(\frac{2\pi \cos(2\pi x)}{(1+x)^2} - \frac{2 \sin(2\pi x)}{(1+x)^3} \right) \\
 & + t^2(2 - \sin(tx)) \left(4\pi^2 \frac{\sin(2\pi x)}{(1+x)^2} + \frac{8\pi \cos(2\pi x)}{(1+x)^3} - \frac{6 \sin(2\pi x)}{(1+x)^4} \right),
 \end{aligned}$$

with the exact solution $u(x, t) = t^2 \frac{\sin(2\pi x)}{(1+x)^2}$.

In Table 1, we select $\tau = h^2$ ($K = N^2$), since, from our theoretical estimates, the error in the L^2 norm is expected to be $\mathcal{O}(\tau^2 + h^4)$ when $r = 3$. Just as we hope, the results in Table 1 demonstrate the expected convergence rates of 4 order in space and 2 in time for different α ($\alpha = 0.15, 0.5, 0.95$).

We now verify the temporal accuracy and convergence rates for our proposed method, and select $\tau = h$ ($K = N$), so that the error stemming from the spatial approximation is negligible. Table 2 verifies 2 order accuracy in time for all four different α ($\alpha = 0.1, 0.5, 0.99$), which are in keeping with the theoretical predictions.

By selecting $\tau = h^{3/2}$ and different α ($\alpha = 0.01, 0.4, 0.7, 0.9$), Table 3 indicates H^1 errors and convergence rates in spatial direction. The convergence rate of 3 order matches that of the theoretical one.

Example 2 We consider the following problem similar to Chen et al. (2016):

$$\begin{cases}
 u_t + {}_0^C D_t^\alpha u - (2 - \sin(tx))u_{xx} + t \cos(tx)u_x + (2 - \cos(tx))u = f(x, t), \\
 u(x, 0) = 0, \quad x \in \Omega, \\
 u(x, t) = 0, \quad (x, t) \in \partial\Omega \times (0, T],
 \end{cases}$$

where $\Omega = [0, 1], T = 1$:

$$\begin{aligned}
 f(x, t) = & (\Gamma(2 + \alpha)t + (1 + \alpha)t^\alpha + (2 - \cos(tx))t^{1+\alpha}) x(1-x)e^{-x} \\
 & + t^3 \cos(tx)(2 - \sin(tx))(x^2 - 5x + 4)e^{-x}t^{1+\alpha} \\
 & + t \cos(tx)(x^2 - 3x + 1)e^{-x}t^{1+\alpha}.
 \end{aligned}$$

Table 2 L^2 and L^∞ errors and convergence rates in temporal direction with $\tau = h$ for Example 1

α	N	L^2 error	Rate	L^∞ error	Rate
$\alpha = 0.1$	10	9.1750e-04		1.6547e-03	
	20	2.2990e-04	1.9967	4.1500e-04	1.9954
	40	5.7374e-05	2.0025	1.0305e-04	2.0098
	80	1.4337e-05	2.0007	2.5776e-05	1.9992
	160	3.5839e-06	2.0001	6.4429e-06	2.0002
	320	8.9593e-07	2.0001	1.6107e-06	2.0000
$\alpha = 0.5$	10	9.0771e-04		1.6358e-03	
	20	2.2815e-04	1.9922	4.1181e-04	1.9899
	40	5.6949e-05	2.0022	1.0228e-04	2.0095
	80	1.4232e-05	2.0005	2.5578e-05	1.9995
	160	3.5577e-06	2.0001	6.3943e-06	1.9856
	320	8.8939e-07	2.0001	1.5984e-06	2.0002
$\alpha = 0.99$	10	9.0174e-04		1.6228e-03	
	20	2.3027e-04	1.9694	4.1554e-04	1.9654
	40	5.7493e-05	2.0019	1.0326e-04	2.0087
	80	1.4368e-05	2.0005	2.5832e-05	1.9991
	160	3.5917e-06	2.0001	6.4509e-06	2.0002
	320	8.9787e-07	2.0001	1.6142e-06	2.0000

Table 3 H^1 errors and convergence rates with $\tau = h^{\frac{3}{2}}$ for Example 1

α	N	H^1 error	Rate	α	N	H^1 error	Rate
$\alpha = 0.01$	4	8.9442e-03		$\alpha = 0.4$	4	8.7744e-03	
	9	7.5363e-04	3.0506		9	7.3900e-04	3.0512
	16	1.3321e-04	3.0120		16	1.3062e-04	3.0120
	25	3.4856e-05	3.0041		25	3.4175e-05	3.0043
	36	1.1665e-05	3.0019		36	1.1437e-05	3.0020
$\alpha = 0.7$	4	8.6247e-03		$\alpha = 0.9$	4	8.5192e-03	
	9	7.2610e-04	3.0517		9	7.1701e-04	3.0520
	16	1.2832e-04	3.0123		16	1.2671e-04	3.0123
	25	3.3575e-05	3.0042		25	3.3152e-05	3.0043
	36	1.1236e-05	3.0020		36	1.1095e-05	3.0019

Tables 4, 5, 6 show the errors and convergence rates in three discrete norms for Example 2.

For the fractional order $\alpha = 0.25, 0.5, 0.95$, Table 4 shows the L^2 and L^∞ errors and convergence rates, and verifies that the space convergence rate is 4 and time convergence rate is 2 for each α . It is obvious that the numerical convergence order matches well with the theoretical results.

In Table 5, for the fractional order $\alpha = 0.01, 0.35, 0.65, 0.99$, we present the convergence order in temporal direction. It is easy to conclude that the method is convergent and the convergence order in time is 2 corresponding to each α .

We show the errors in H^1 norm for $\alpha = 0.01, 0.3, 0.6, 0.8$ in Table 6. It is clear that the convergence rate is three, which is the same as theoretically claimed.

Table 4 L^2 and L^∞ errors and convergence rates in spatial and temporal directions with $\tau = h^2$ for Example 2

α	N	L^2 error	Rate	L^∞ error	Rate
$\alpha = 0.25$	5	6.2814e-06		8.9435e-06	
	10	3.9061e-07	4.0073	5.4825e-07	4.0279
	20	2.2818e-08	4.0975	3.2192e-08	4.0901
	40	1.1431e-09	4.3191	1.6557e-09	4.2812
$\alpha = 0.5$	5	1.6796e-05		2.3666e-05	
	10	1.0516e-06	3.9975	1.4738e-06	4.0052
	20	6.5130e-08	4.0131	9.1297e-08	4.0128
	40	3.9931e-09	4.0277	5.6118e-09	4.0240
$\alpha = 0.95$	5	4.2702e-05		5.9971e-05	
	10	2.6753e-06	3.9965	3.7487e-06	3.9998
	20	1.6723e-07	3.9998	2.3430e-07	4.0000
	40	1.0452e-08	4.0000	1.4656e-08	3.9988

Table 5 L^2 and L^∞ errors and convergence rates in temporal direction with $\tau = h$ for Example 2

α	N	L^2 error	Rate	L^∞ error	Rate
$\alpha = 0.01$	10	1.5366e-06		2.4599e-06	
	20	3.7003e-07	2.0540	4.9885e-07	2.3019
	40	9.2193e-08	2.0049	1.2909e-07	1.9502
	80	2.3003e-08	2.0028	3.2270e-08	2.0001
	160	5.7098e-09	2.0103	8.0153e-09	2.0094
	320	1.4654e-09	1.9621	2.0292e-09	1.9818
$\alpha = 0.35$	10	6.8788e-05		1.0268e-04	
	20	1.7205e-05	1.9993	2.3984e-05	2.0980
	40	4.2862e-06	2.0051	6.0150e-06	1.9954
	80	1.0651e-06	2.0087	1.4955e-06	2.0079
	160	2.6361e-07	2.0145	3.7045e-07	2.0133
	320	6.4898e-08	2.0222	9.1273e-08	2.0210
$\alpha = 0.65$	10	1.5480e-04		2.2205e-04	
	20	3.8822e-05	1.9955	5.4358e-05	2.0303
	40	9.7038e-06	2.0003	1.3618e-05	1.9970
	80	2.4246e-06	2.0008	3.4034e-06	2.0005
	160	6.0565e-07	2.0012	8.5028e-07	2.0010
	320	1.5131e-07	2.0010	2.1240e-07	2.0012
$\alpha = 0.99$	10	2.8168e-04		3.9743e-04	
	20	7.0636e-05	1.9956	9.9034e-05	2.0047
	40	1.7659e-05	2.0000	2.4794e-05	1.9979
	80	4.4148e-06	2.0000	6.1990e-06	1.9999
	160	1.1037e-06	2.0000	1.5500e-06	1.9998
	320	2.7597e-07	1.9998	3.8753e-07	1.9999

Table 6 H^1 errors and convergence rates with $\tau = h^{\frac{3}{2}}$ for Example 2

α	N	H^1 error	Rate	α	N	H^1 error	Rate
$\alpha = 0.01$	4	7.7151e-06		$\alpha = 0.3$	4	7.0090e-05	
	9	7.3209e-07	2.9041		9	6.2287e-06	2.9850
	16	1.3178e-07	2.9803		16	1.0847e-06	3.0378
	25	3.4849e-08	3.0456		25	2.7059e-07	3.1111
	36	1.1814e-08	2.8867		36	8.3719e-08	3.2172
$\alpha = 0.6$	4	1.8146e-04		$\alpha = 0.8$	4	2.7372e-04	
	9	1.6709e-05	2.9412		9	2.5361e-05	2.9335
	16	2.9941e-06	2.9882		16	4.5552e-06	2.9841
	25	7.8443e-07	3.0013		25	1.1969e-06	2.9948
	36	2.6201e-07	3.0073		36	4.0112e-07	2.9981

Example 3 We consider the following problem Chen et al. (2016):

$$\begin{cases} {}_0^C D_t^\alpha u - (2 - \sin(tx))u_{xx} + (2 - \cos(tx))u = f(x, t), \\ u(x, 0) = 0, \quad x \in [0, 1], \\ u(0, t) = u(1, t) = 0, \quad t \in (0, 1], \end{cases}$$

with

$$f(x, t) = (\Gamma(2 + \alpha)t + (2 - \cos(tx))t^{1+\alpha})x(1 - x)e^{-x} + t^3 \cos(tx)(2 - \sin(tx))(x^2 - 5x + 4)e^{-x}t^{1+\alpha}.$$

In this example, by choosing the same parameter h , τ and α as in Chen et al. (2016), we compare the numerical results of our scheme with the method in Chen et al. (2016). To eliminate the contamination of the spatial error, we choose $h = 1/125$, which is large enough as the solution is analytic. Tables 7, 8 display L^2 and L^∞ errors and the convergence orders with $\alpha = 0.1, 0.5, 0.9$, respectively. The last two columns of Tables 7 and 8 present the numerical results obtained in Chen et al. (2016). From Tables 7 and 8, we can see that the present method have similar accuracy and convergence order in time as reference Chen et al. (2016).

In the following Example 4, we mainly test problem based on the Gaussian pulse and the noise effect to show the efficiency of the developed technique.

Example 4 Let $\Omega = [0, 1]$, $T = 1$, we consider the following problem:

$$\begin{cases} u_t + {}_0^C D_t^\alpha u - (2 - \sin(tx))u_{xx} + t \cos(tx)u_x + (2 - \cos(tx))u = f(x, t), \\ u(x, 0) = 0, \quad x \in \Omega, \\ u(x, t) = 0, \quad (x, t) \in \partial\Omega \times (0, T], \end{cases}$$

with the exact solution $u(x, t) = t^{2+\alpha} e^{-\frac{(x-0.5)^2}{\beta}} \sin(\pi x)$, where β is small parameter.

In Fig. 1, we draw the surface figures of the exact solution u and the numerical solution u_h with $h = 1/40$, $\tau = 1/1600$, $\alpha = 0.5$, and $\beta = 0.01$, respectively. We can clearly see that the exact solution u can be simulated well by the approximation solution u_h for our discrete

Table 7 Comparison of L^2 errors and convergence rate for Example 3 with $1/h = 125$

α	$1/\tau$	Present scheme	Rate	Method in Chen et al. (2016)	Rate in Chen et al. (2016)
$\alpha = 0.1$	10	1.6793e-05		1.7043e-05	
	20	4.0355e-06	2.0570	4.2473e-06	2.0046
	40	9.9656e-07	2.0177	1.0562e-06	2.0077
	80	2.4558e-07	2.0208	2.6227e-07	2.0097
	160	5.9759e-08	2.0390	6.5079e-08	2.0108
	320	1.4171e-08	2.0762	1.6144e-08	2.0111
$\alpha = 0.5$	10	1.0867e-04		3.2094e-04	
	20	2.7249e-05	1.9957	8.0434e-05	1.9964
	40	6.8041e-06	2.0017	2.0169e-05	1.9957
	80	1.6973e-06	2.0032	5.0559e-06	1.9961
	160	4.2295e-07	2.0047	1.2668e-06	1.9968
	320	1.0524e-07	2.0068	3.1723e-07	1.9976
$\alpha = 0.9$	10	2.4508e-04		9.6360e-04	
	20	6.1448e-05	1.9958	2.4051e-04	2.0023
	40	1.5364e-05	1.9998	6.0069e-05	2.0014
	80	3.8409e-06	2.0000	1.5006e-05	2.0011
	160	9.6023e-07	2.0000	3.7492e-06	2.0009
	320	2.4006e-07	2.0000	9.3680e-07	2.0008

Table 8 Comparison of L^∞ errors and convergence rate for Example 3 with $1/h = 125$

α	$1/\tau$	Present scheme	Rate	Method in Chen et al. (2016)	Rate in Chen et al. (2016)
$\alpha = 0.1$	10	2.6974e-05		1.2417e-05	
	20	5.5287e-06	2.2866	3.0903e-06	2.0065
	40	1.3980e-06	1.9836	7.6774e-07	2.0091
	80	3.4505e-07	2.0185	1.9049e-07	2.0109
	160	8.4135e-08	2.0360	4.7238e-08	2.0117
	320	2.0035e-08	2.0702	1.1712e-08	2.0120
$\alpha = 0.5$	10	1.5913e-04		2.3983e-04	
	20	3.8136e-05	2.0610	6.0116e-05	1.9962
	40	9.5508e-06	1.9975	1.5075e-05	1.9956
	80	2.3829e-06	2.0029	3.7790e-06	1.9961
	160	5.9389e-07	2.0045	9.4683e-07	1.9968
	320	1.4781e-07	2.0065	2.3711e-07	1.9976
$\alpha = 0.9$	10	3.4733e-04		7.2366e-04	
	20	8.6260e-05	2.0095	1.8070e-04	2.0017
	40	2.1574e-05	1.9994	4.5145e-05	2.0010
	80	5.3934e-06	2.0000	1.1281e-05	2.0007
	160	1.3484e-06	1.9999	2.8192e-06	2.0005
	320	3.3709e-07	2.0000	7.0460e-07	2.0004

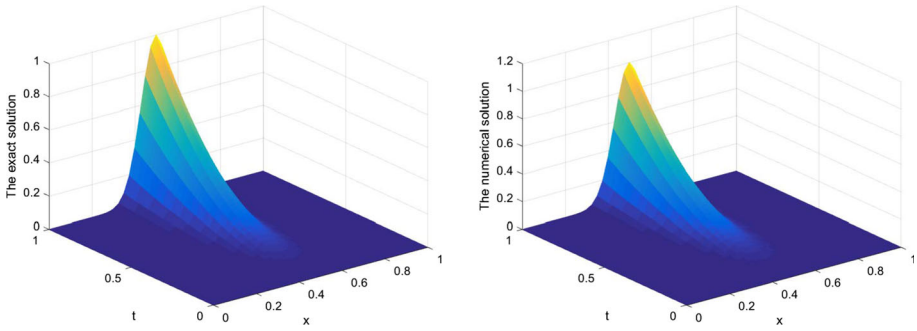
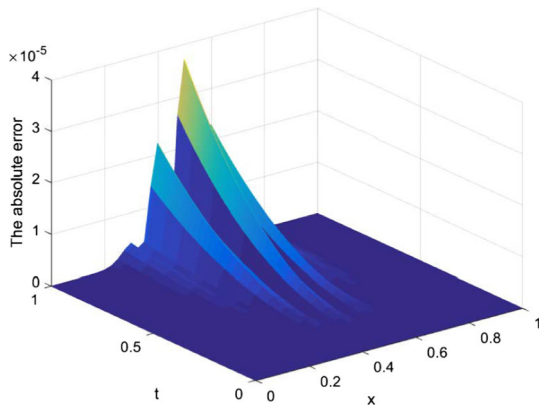


Fig. 1 Left: the exact solution. Right: the numerical solution

Fig. 2 The absolute error of the numerical solution at $\alpha = 0.5$ and $\tau^2 = h^4 = \frac{1}{1600}$ for Example 4



scheme in this case. In Fig. 2, we give the error surface figure for $|u - u_h|$. From the error figure, we can find that our numerical method can solve well the numerical solution in this case.

5 Conclusion

In the present work, we have developed an effective Crank–Nicolson OSC scheme for fractional-order mobile–immobile equation with variable coefficients. It is proved that our proposed fully methods are of optimal order in certain H_j ($j = 0, 1$) norms. Also, L^∞ estimates in space are derived. Some numerical examples have been carried out to verify the accuracy and efficiency of Crank–Nicolson OSC scheme.

Acknowledgements Many thanks to Prof. Graeme Fairweather for stimulating discussions and for his constant encouragement and support.

Compliance with ethical standards

Conflict of interest The authors declare to have no conflict of interest.

References

- Bialecki B (1998) Convergence analysis of orthogonal spline collocation for elliptic boundary value problems. *SIAM J. Numer. Anal.* 35:617–631
- Bialecki B, Fernandes RI (1993) Orthogonal spline collocation Laplace-modified and alternating-direction methods for parabolic problems on rectangles. *Math. Comput.* 60:545–573
- Chen H, Lü SJ, Chen WP (2016) Spectral and pseudospectral approximations for the time fractional diffusion equation on an unbounded domain. *J. Comput. Appl. Math.* 304:43–56
- Chen HB, Gan SQ, Xu D, Liu QW (2016) A second-order BDF compact difference scheme for fractional-order Volterra equations. *Int. J. Comput. Math.* 93:1140–1154
- Cui MR (2015) Compact exponential scheme for the time fractional convection–diffusion reaction equation with variable coefficients. *J. Comput. Phys.* 280:143–163
- Fernandes RI, Fairweather G (1993) Analysis of alternating direction collocation methods for parabolic and hyperbolic problems in two space variables. *Numer. Methods Partial Differ. Equ.* 9:191–211
- He DD, Pan KJ (2017) An unconditionally stable linearized CCD–ADI method for generalized nonlinear Schrödinger equations with variable coefficients in two and three dimensions. *Comput. Math. Appl.* 73:2360–2374
- He DD, Pan KJ (2018) An unconditionally stable linearized difference scheme for the fractional Ginzburg–Landau equation. *Numer. Algorithms* 79:899–925
- Jiang YJ (2015) A new analysis of stability and convergence for finite difference schemes solving the time fractional Fokker–Planck equation. *Appl. Math. Model.* 39:1163–1171
- Liu Z, Li X (2018) A Crank–Nicolson difference scheme for the time variable fractional mobile–immobile advection–dispersion equation. *J. Appl. Math. Comput.* 56:391–410
- Liu F, Zhuang P, Burrage K (2012) Numerical methods and analysis for a class of fractional advection–dispersion models. *Comput. Math. Appl.* 64:2990–3007
- Liu Q, Liu F, Turner I, Anh V, Gu YT (2014) A RBF meshless approach for modeling a fractal mobile/immobile transport model. *Appl. Math. Comput.* 226:336–347
- Liu Y, Du YW, Li H, Li JC, He S (2015) A two-grid mixed finite element method for a nonlinear fourth-order reaction diffusion problem with time-fractional derivative. *Comput. Math. Appl.* 70:2474–2492
- Percell P, Wheeler MP (1980) A C^1 finite element collocation method for elliptic partial differential equations. *SIAM J. Numer. Anal.* 17:923–939
- Tian WY, Zhou H, Deng WH (2015) A class of second order difference approximations for solving space fractional diffusion equations. *Math. Comput.* 84:1703–1727
- Wang Z, Vong S (2014) Compact difference schemes for the modified anomalous fractional sub-diffusion equation and the fractional diffusion-wave equation. *J. Comput. Phys.* 277:1–15
- Wang FL, Zhao YM, Chen C, Wei YB, Tang YF (2019) A novel high-order approximate scheme for two-dimensional time-fractional diffusion equations with variable coefficient. *Comput. Math. Appl.* 78:1288–1301
- Wei LL (2017) Analysis of a new finite difference/local discontinuous Galerkin method for the fractional diffusion-wave equation. *Appl. Math. Comput.* 304:180–189
- Wei LL (2018) Analysis of a new finite difference/local discontinuous Galerkin method for the fractional Cattaneo equation. *Numer. Algorithms* 77:675–690
- Yan Y, Fairweather G (1992) Orthogonal spline collocation methods for some partial integro-differential equations. *SIAM J. Numer. Anal.* 29:755–768
- Yang XH, Zhang HX, Zhang Q, Yuan GW, Sheng ZQ (2019) The finite volume scheme preserving maximum principle for two-dimensional time-fractional Fokker–Planck equations on distorted meshes. *Appl. Math. Lett.* 97:99–106
- Zhang H, Liu F, Phanikumar MS, Meerschaert MM (2013) A novel numerical method for the time variable fractional order mobile–immobile advection–dispersion model. *Comput. Math. Appl.* 66:693–701
- Zhang HX, Yang XH, Xu D (2019) A high-order numerical method for solving the 2D fourth-order reaction–diffusion equation. *Numer. Algorithms* 80:849–877